# The Influence of Hydrogen on Defects of In–Ga–Zn–O Semiconductor Thin-Film Transistors With Atomic-Layer Deposition of $Al_2O_3$

Taeho Kim, Yunyong Nam, Jihyun Hur, Sang-Hee Ko Park, and Sanghun Jeon, *Senior Member, IEEE*

***Abstract*— Hydrogen plays a crucial role in several oxide semiconductors, where the amount of hydrogen significantly influences the device performance. Thus, its manipulation in oxide semiconductors is important for device performance. In our investigation, we studied the effect of hydrogen on defects in In–Ga–Zn–O semiconductor thin-film transistors (TFTs), as it varies with $Al_2O_3$ atomic layer deposition temperature. We found that the total trap-density ($N_{tot}$) extracted by the sub-threshold slope and the trap density ($N_t$) measured by low-frequency noise (LFN) as well as the density-of-states analyzed by capacitance–voltage decreased with increasing amounts of hydrogen in the oxide semiconductor. Given that LFN data show that mobility fluctuation is the major origins of noise and the front channel of TFT is a major carrier transport region, our results indicate that hydrogen effectively passivates the defects in front channel of oxide semiconductor and contributes to achieving superior device performance.**

***Index Terms*— Defects, hydrogen, indium gallium zinc oxide (IGZO), low-frequency noise (LFN), thin-film transistors (TFTs).**

## I. Introduction

AMORPHOUS indium gallium zinc oxide semiconductors (*a*-IGZO) have gained noteworthy attention in thin-film transistor (TFT) community owing to their excellent electrical, optical and physical properties [1]–[11]. However, the stability of *a*-IGZO TFTs remains the most important and critical issue because it has a certain number of defects in semiconductor. Thus, both the defects in *a*-IGZO and their implications for *a*-IGZO device performance need to be understood [6]–[9]. Hydrogen tends to exhibit strong bonding with oxygen in oxide semiconductors owing to the chemical natures of both elements [6]. Thus, hydrogen is always found in oxide semiconductors and behaves as a defect passivator or shallow donor, depending on the amounts of hydrogen and oxygen [6]–[8]. Recently, various groups have reported on the role of hydrogen as a defect passivator [8], [9], [12], leading to improvement in the devices. However, the effect of hydrogen on defects in IGZO and its influence on device performance are neither clearly examined nor fully understood. In our investigation, we studied the influence of hydrogen on defects in *a*-IGZO TFTs. The amount of hydrogen was adjusted by varying the deposition temperature ($T_{depo}$) of the atomic layer deposition (ALD) gate insulator. In order to examine the defect densities, we employed various device analysis methods, such as DC current voltage (I–V) and low-frequency noise (LFN), as well as multi-frequency capacitance–voltage (C–V) measurements [13]–[17]. Via systematic analysis, we were able to understand the influence of hydrogen on defects in *a*-IGZO TFT and its implication for the device performance.

Manuscript received June 11, 2016; revised July 5, 2016; accepted July 14, 2016. Date of current version August 23, 2016. This work was supported by the National Research Foundation of Korea (NRF) grant funded by the Korean Government (MEST) (2014R1A2A2A01006541). This work was performed, supported by Samsung Display Co., Ltd. The review of this letter was arranged by Editor W. S. Wong.

T. Kim, J. Hur, and S. Jeon are with the Department of Applied Physics, Korea University, Sejong City 339-700, South Korea (e-mail: jeonsh@korea.ac.kr).

Y. Nam and S.-H. K. Park are with Department of Materials Science and Engineering, Korea Advanced Institute of Science and Technology, Daejeon 34141, South Korea (e-mail: shkp@kaist.ac.kr).

Color versions of one or more of the figures in this letter are available online at http://ieeexplore.ieee.org.

Digital Object Identifier 10.1109/LED.2016.2594258

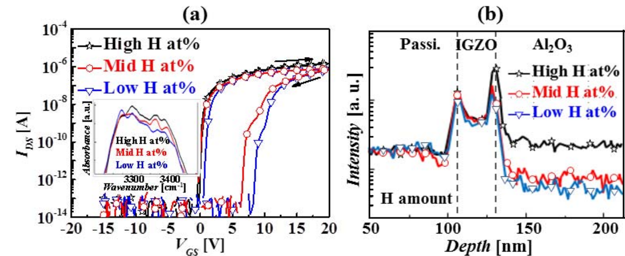


Fig. 1. (a) Transfer ($I_{DS}$–$V_{GS}$) characteristics of *a*-IGZO TFTs with different hydrogen amount. Inset shows Fourier-Transform Infrared Data. (b) SIMS depth profile of hydrogen in *a*-IGZO TFTs with $Al_2O_3$.

## II. Experiment

We prepared bottom-gated TFTs with *a*-IGZO semiconductor materials composited of 1:1:2.5 for cation elements and InSnO source/drain electrodes by RF sputtering method at room temperature and photolithography technique. For a gate insulator, 176nm-thick $Al_2O_3$ dielectrics were prepared by the ALD method at deposition temperatures of 150, 250 and 300 °C, respectively. For hydrogen diffusion step, we performed annealing process at 250 °C in vacuum. The transfer ($I_{DS}$–$V_{GS}$) characteristics of *a*-IGZO TFTs were evaluated at $V_{DS}$ of 0.1 V [Fig. 1(a)]. The threshold voltage ($V_{TH}$) was determined by the $V_{GS}$ that induced an $I_{DS}$ of W/L × 10 nA at a $V_{DS}$ of 0.1 V. Fourier transform infrared (FTIR) spectroscopy study was performed to detect the amount of hydrogen as seen in the inset. The LFN was measured using a semiconductor device analyzer with an AC-waveform generator. The multi-frequency C–V was measured at frequencies. Medium and

0741-3106 © 2016 IEEE. Personal use is permitted, but republication/redistribution requires IEEE permission.
See http://www.ieee.org/publications_standards/publications/rights/index.html for more information.

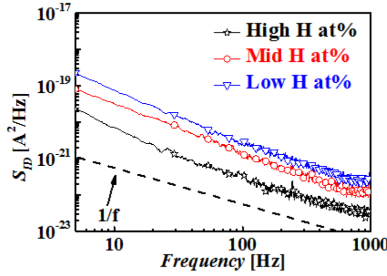


Fig. 2. Noise spectral density ($S_{ID}$) versus frequency for *a*-IGZO TFTs with hydrogen amount.

low H at% samples shows large $\Delta V_{th}$ [Fig. 1a]. In order to ensure reliable noise and multi-frequency C-V measurements, we manipulated the bias stress condition as a pre-measurement step. Then, $\Delta$ $V_{th}$ was made to be negligible. The hydrogen amount in *a*-IGZO TFT with $Al_2O_3$ was detected by Secondary Ion Mass Spectroscopy (SIMS). As seen in the Fig. 1 (b). SIMS data on *a*-IGZO with $Al_2O_3$ $T_{depo}$ of 150, 250 and 300 °C present high, middle and low hydrogen (H) concentration in the front channel and front/back interfaces. The H at% was decreased with increasing $T_{depo}$, which is consistent with FTIR study.

## III. Results and Discussion

As illustrated in Fig. 1(a), the transistor characteristics of an *a*-IGZO TFT are influenced by the $T_{depo}$ of $Al_2O_3$ and the H at%. A high H at% *a*-IGZO TFT with $Al_2O_3$ at 150 °C presents a significantly high $\mu_{linear}$ (17.8 cm$^2$/V-s), low sub-threshold slope ($S$) (0.12 V/dec) and negligible hysteresis (0.1 V) as compared to a middle H at% TFT with 250 °C $Al_2O_3$ ($\mu_{linear}$ of 8.5 cm$^2$/V-s, $S$ of 0.17 V/dec. and hysteresis of 7 V) and a low H at% TFT with 300 °C $Al_2O_3$ ($\mu_{linear}$ of 2.1 cm$^2$/V-s, $S$ of 0.22 V/dec. and hysteresis of 11.3 V). The $S$ value can be changed to the total trap density ($N_{tot}$),

$$N_{tot} = N_{bulk} + N_{it} = \left(\frac{S\log(e)}{\frac{kT}{q}} - 1\right)\frac{C_{ox}}{q} \tag{1}$$

where $N_{bulk}$ is the bulk trap density, $N_{it}$ is the interface trap density, $kT$ is thermal energy, $q$ is the elementary charge and $C_{ox}$ is the gate insulator capacitance [18], [19]. High, middle and low H at% *a*-IGZO TFTs present values of $N_{tot}$ of $4.81 \times 10^{11}$, $8.55 \times 10^{11}$ and $1.34 \times 10^{12}$ cm$^{-2}$eV$^{-1}$, respectively. The $N_{tot}$ of the low H at% TFT is 2.8 times higher than that of the high H at% TFT.

To examine further the defect densities and to probe the carrier transport mechanisms of TFT devices, we measured LFN characteristics for various H at% a-IGZO TFTs. Figure 2 shows noise spectral densities ($S_{ID}$) versus gate overdrive voltages $|V_{GS} - V_{TH}|$ measured at $V_{GS} - V_{TH} = 1$ V and $V_{DS} = 1$ V. The magnitude of the measured $S_{ID}$ fits well to the $1/f^{\gamma}$ relationship, following the classical $1/f$ noise theory [13]. The method to find the dominant mechanism is to observe the slope of $S_{ID}/I_D^2$ versus $|V_{GS} - V_{TH}|$ [13]–[16]. The carrier number fluctuation ($\Delta$n) model predicts $S_{ID}/I_D^2 \propto |V_{GS} - V_{TH}|^{-2}$, while the mobility fluctuation ($\Delta\mu$) model follows $S_{ID}/I_D^2 \propto |V_{GS} - V_{TH}|^{-1}$ [13]–[16]. Thus, the dependency of $S_{ID}/I_D^2$ on $|V_{GS} - V_{TH}|$ was assessed in detail to determine the carrier transport mechanism of various H at% *a*-IGZO TFTs

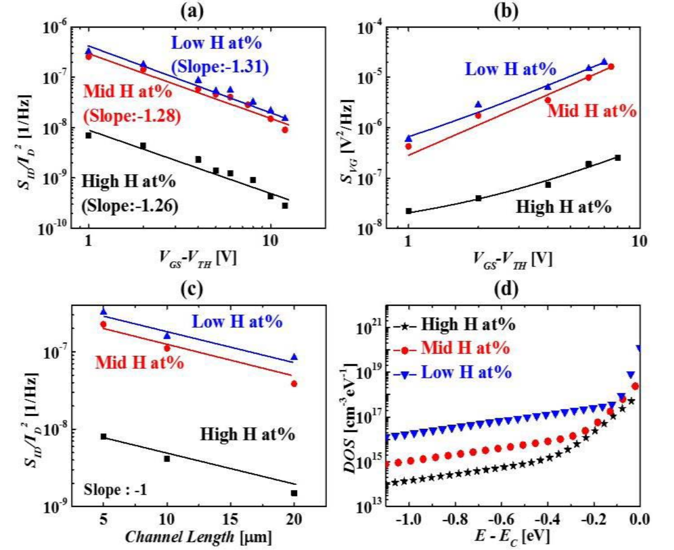


Fig. 3. (a) Normalized noise spectral density ($S_{ID}/I_D^2$) versus gate overdrive voltage, (b) voltage spectral density ($S_{VG}$) versus gate overdrive voltage at $V_{DS} = 1$ V and $f = 20$ Hz., (c) normalized noise spectral density ($S_{ID}/I_D^2$) versus gate length at $V_{DS} = 1$ V and $f = 20$ Hz and (d) extracted density of states of *a*-IGZO TFTs with different hydrogen amount.

as seen in Fig. 3(a). The normalized $S_{ID}$ varies as $|V_{GS} - V_{TH}|^{-m}$, with m in the range of $1 < m < 1.4$ for all devices. The $\Delta\mu$ model is the major noise mechanism in *a*-IGZO TFTs. However, when considering the deviations in m for all *a*-IGZO TFTs from the predicted value of 1 using the $\Delta\mu$ model, it was not obvious enough that $\Delta\mu$ comprises the entire source of the LFN. It was reasonable to use the unified $\Delta\mu$-$\Delta$ n model to determine the source of LFN [13]–[16]. From the theory unifying $\Delta$ n with correlated $\Delta\mu$, we can define the input-referred voltage spectral densities ($S_{VG} = S_{ID}/G_M^2$) and plot $S_{VG}$ versus $|V_{GS} - V_{TH}|$ as seen in Fig. 3(b).

$$S_{VG} = S_{VFB}\left[1 + \alpha\mu_{eff}C_{ox}\left(V_{GS} - V_{TH}\right)\right]^2 \tag{2}$$

and

$$S_{VFB} = \frac{\lambda kTq^2N_t}{fWLC_{ox}^2} \tag{3}$$

where $S_{VFB}$ is the flat-band voltage noise density, $\alpha$ is the Coulomb-scattering coefficient, $\mu_{eff}$ is the effective mobility, $C_{ox}$ is the gate oxide capacitance, $\lambda$ is the tunneling attenuation coefficient (i.e., ~0.11 nm for $Al_2O_3$), $k$ is the Boltzmann constant, $T$ is the temperature, $q$ is the elementary charge and $N_t$ is the trap density, $f$ is the frequency [20].

Thus, all *a*-IGZO TFTs devices follow the $\Delta$ n model with $\alpha = 7.55 \times 10^5$ Vs/C (high H at%), $8.05 \times 10^5$ Vs/C (mid H at%), and $1.83 \times 10^6$ Vs/C (low H at%). The extracted $S_{VFB}$ and $N_t$ of *a*-IGZO TFTs are $8.19 \times 10^{-10}$ V$^2$/Hz and $1.17 \times 10^{18}$ cm$^{-3}$ eV$^{-1}$ (high H at%), $3.35 \times 10^{-9}$ V$^2$/Hz and $4.67 \times 10^{18}$ cm$^{-3}$ eV$^{-1}$ (mid H at%), and $1.87 \times 10^{-8}$ V$^2$/Hz and $3.06 \times 10^{19}$ cm$^{-3}$ eV$^{-1}$ (low H at%), respectively. We should note that the $N_t$ value of the low H at% TFT is about one order of magnitude higher than that of the high H at% TFT.

In order to classify the channel noise and contact noise, the length effects of LFN data were monitored. The effect of channel length (L) on the LFNs of various H at% *a*-IGZO TFTs are presented in Fig. 3(c). The tendency and the value are

TABLE I
THE EXTRACTED MODEL PARAMETERS OF DENSITY OF STATES

| G.I. deposition temp. (Hydrogen at%) | $N_{TA}$ ($cm^{-3}eV^{-1}$) | $kT_{TA}$ (eV) | $N_{DA}$ ($cm^{-3}eV^{-1}$) | $kT_{DA}$ (eV) |
|---|---|---|---|---|
| 150℃ (High) | $1.1x10^{18}$ | 0.05 | $4x10^{15}$ | 0.3 |
| 250℃ (Mid) | $4x10^{18}$ | 0.04 | $3x10^{16}$ | 0.3 |
| 300℃ (Low) | $1.2x10^{20}$ | 0.015 | $5x10^{17}$ | 0.3 |

also observed in all devices with L from 5–20 $\mu$m. When the channel noise governs, normalized $S_{ID}$ is proportional to $L^{-1}$. When the contact noise is the dominant source of LFN, then the normalized $S_{ID}$ is proportional to $L^{-2}$ [15], [16]. In our investigation, the slope of the normalized $S_{ID}$ versus $L_G$ for all tested *a*-IGZO TFTs was found to be around −1, which indicates that LFNs were mainly generated in the channel region [Fig. 3(c)].

Since the sub-gap density-of-states (DOS) of oxide TFTs are the most important parameters for determining both device performance and reliability, we examined the sub-gap DOS of various H at% *a*-IGZO TFTs by multi-frequency C–V technique. Here, we extracted the f-independent gate capacitance from the measured multi-frequency C–V data [17].

As a result, we obtained the DOS for three different multi-frequency combinations with $\omega_1$, $\omega_2$ and $\omega_3$. Table 1 presents the sub-gap DOS of high H at%, medium H at% and low H at% *a*-IGZO TFTs, clearly depicting the superposition of exponential tail states and exponential deep states.

$$g\,(E) = N_{TA} \times \exp\left(\frac{(E - E_c)}{kT_{TA}}\right) + N_{DA} \times \exp\left(\frac{(E - E_c)}{kT_{DA}}\right) \quad (4)$$

where the extracted model parameters are the acceptor-like tail-state density ($N_{TA}$), the acceptor-like deep-state density ($N_{DA}$), the acceptor-like tail-state energy ($kT_{TA}$) and the acceptor-like deep-state energy ($kT_{DA}$) [21]–[23]. We need to notice that the extracted sub-gap DOS of oxide TFTs is influenced by the amount of hydrogen in *a*-IGZO TFTs. This is consistent with the $N_{tot}$ values extracted by $S$ and the $N_t$ obtained from LFN data. Consistent with the sub-gap DOS data, positive and negative bias temperature stress tests on a-IGZO TFTs show that higher hydrogen at% correlates with smaller threshold voltage shifts.

While bottom-gate TFT is fabricated, the active IGZO layer was deposited via sputtering on top of the gate insulator. Therefore, the surface of the gate dielectric in the vicinity of the front IGZO channel was mainly damaged by the plasma. In addition, during the CVD process for the $SiO_2$ passivation layer and/or sputtering process in oxygen ambient, excess oxygen can be introduced to the IGZO layer and oxygen interstitial states may degrade the quality of the IGZO TFTs. Those states can be passivated by the hydrogen atoms diffused from the gate insulator during post-annealing.

## IV. SUMMARY

We studied the effect of hydrogen on defects of *a*-IGZO TFTs. As presented in SIMS and FTIR results, the hydrogen amount was varied with the deposition temperature of ALD $Al_2O_3$. It decreases with increasing $Al_2O_3$ $T_{depo}$ (150, 250 and 300 °C). We found that the $N_{tot}$ extracted by the $S$ of the DC I–V curve and the $N_t$ by LFN as well as the DOS by C–V were noticeably reduced when increasing the hydrogen amount in *a*-IGZO TFTs. All these results indicate that hydrogen effectively passivates defects in the front channel-interface of TFT and reduces lattice scattering events. Even if the role of hydrogen has been controversial in past works, our study presents the finding that hydrogen plays a helpful role in ALD $Al_2O_3$ stacked *a*-IGZO TFTs.

## REFERENCES


[1] S. J. Kim, S. Yoon, and H. J. Kim, “Review of solution-processed oxide thin-film transistors,” *Jpn. J. Appl. Phys.*, vol. 53, no. 2S, pp. 02BA02-1–02BA02-10, Feb. 2014.

[2] K. Nomura, H. Ohta, A. Takagi, T. Kamiya, M. Hirano, and H. Hosono, “Room-temperature fabrication of transparent flexible thin-film transistors using amorphous oxide semiconductors,” *Nature*, vol. 432, no. 7016, pp. 488–492, Nov. 2004.

[3] S. Jeon, S.-E. Ahn, I. Song, C. J. Kim, U.-I. Chung, E. Lee, I. Yoo, A. Nathan, S. Lee, K. Ghaffarzadeh, J. Robertson, and K. Kim, “Gated three-terminal device architecture to eliminate persistent photoconductivity in oxide semiconductor photosensor arrays,” *Nature Mater.*, vol. 11, no. 4, pp. 301–305, Apr. 2012.

[4] S. Lee, S. Jeon, R. Chaji, and A. Nathan, “Transparent semiconducting oxide technology for touch free interactive flexible displays,” *Proc. IEEE*, vol. 103, no. 4, pp. 644–664, Apr. 2015.

[5] H.-S. Choi and S. Jeon, “Field-induced macroscopic barrier model for persistent photoconductivity in nanocrystalline oxide thin-film transistors,” *Appl. Phys. Lett.*, vol. 104, no. 13, pp. 133507-1–133507-5, Mar. 2014.

[6] C. G. Van de Walle, “Hydrogen as a cause of doping in zinc oxide,” *Phys. Rev. Lett.*, vol. 85, no. 5, pp. 1012–1015, Jul. 2000.

[7] T. Kamiya and H. Hosono, “Material characteristics and applications of transparent amorphous oxide semiconductors,” *NPG Asia Mater.*, vol. 2, no. 1, pp. 15–22, Jan. 2010.

[8] T. Kamiya and H. Hosono, “Roles of hydrogen in amorphous oxide semiconductor,” *ECS Trans.*, vol. 54, no. 1, pp. 103–113, Jun. 2013.

[9] S.-H. K. Park, D.-H. Cho, C.-S. Hwang, S. Yang, M. K. Ryu, C.-W. Byun, S. M. Yoon, W.-S. Cheong, K. I. Cho, and J.-H. Jeon, “Channel protection layer effect on the performance of oxide TFTs,” *ETRI J.*, vol. 31, no. 6, pp. 653–659, Dec. 2009.

[10] S. Jeon, I. Song, S. Lee, B. Ryu, S.-E. Ahn, E. Lee, Y. Kim, A. Nathan, J. Robertson, and U.-I. Chung, “Origin of high photoconductive gain in fully transparent heterojunction nanocrystalline oxide image sensors and interconnects,” *Adv. Mater.*, vol. 26, no. 41, pp. 7102–7109, Nov. 2014.

[11] S. Jeon, A. Benayad, S.-E. Ahn, S. Park, I. Song, C. Kim, and U.-I. Chung, “Short channel device performance of amorphous InGaZnO thin film transistor,” *Appl. Phys. Lett.*, vol. 99, no. 8, p. 082104, Aug. 2011, doi: 10.1063/1.3623426

[12] Y. Hanyu, K. Domen, K. Nomura, H. Hiramatsu, H. Kumomi, H. Hosono, and T. Kamiya, “Hydrogen passivation of electron trap in amorphous In-Ga-Zn-O thin-film transistors,” *Appl. Phys. Lett.*, vol. 103, no. 20, pp. 202114-1–202114-3, Nov. 2013.

[13] S. J. Yun, K.-H. Lee, J. Skarp, H.-R. Kim, and K.-S. Nam, “Dependence of atomic layer-deposited $Al_2O_3$ films characteristics on growth temperature and Al precursors of $Al(CH_3)_3$ and $AlCl_3$,” *J. Vac. Sci. Technol. A*, vol. 15, no. 6, pp. 2993–2997, Nov./Dec. 1997.

[14] J.-M. Lee, W.-S. Cheong, C.-S. Hwang, I.-T. Cho, H.-I. Kwon, and J.-H. Lee, “Low-frequency noise in amorphous indium-gallium-zinc-oxide thin-film transistors,” *IEEE Electron Device Lett.*, vol. 30, no. 5, pp. 505–507, May 2009.

[15] S. Jeon, S. I. Kim, S. Park, I. Song, J. Park, S. Kim, and C. Kim, “Low-frequency noise performance of a bilayer InZnO-InGaZnO thin-film transistor for analog device applications,” *IEEE Electron Device Lett.*, vol. 31, no. 10, pp. 1128–1130, Oct. 2010.

[16] H.-S. Choi, S. Jeon, H. Kim, J. Shin, C. Kim, and U.-I. Chung, “The impact of active layer thickness on low-frequency noise characteristics in InZnO thin-film transistors with high mobility,” *Appl. Phys. Lett.*, vol. 100, no. 17, pp. 173501-1–173501-4, Apr. 2012.

[17] S. Lee, S. Park, S. Kim, Y. Jeon, K. Jeon, J.-H. Park, J. Park, I. Song, C. J. Kim, Y. Park, D. M. Kim, and D. H. Kim, “Extraction of subgap density of states in amorphous InGaZnO thin-film transistors by using multifrequency capacitance–voltage characteristics,” *IEEE Electron Device Lett.*, vol. 31, no. 3, pp. 231–233, Mar. 2010.

[18] H.-S. Choi, S. Jeon, H. Kim, J. Shin, C. Kim, and U.-I. Chung, “Influence of Hf contents on interface state properties in a-HfInZnO thin-film transistors with $SiN_x/SiO_x$ gate dielectrics,” *Appl. Phys. Lett.*, vol. 99, no. 18, pp. 183502-1–183502-3, Oct. 2011.

[19] S. M. Sze and K. K. Ng, *Physics of Semiconductor Devices*, 3rd ed. New York, NY, USA: Wiley, 2007.

[20] H.-S. Choi, S. Jeon, H. Kim, J. Shin, C. Kim, and U.-I. Chung, "Verification of interface state properties of a-InGaZnO thin-film transistors with $SiN_x$ and $SiO_2$ gate dielectrics by low-frequency noise measurements," *IEEE Electron Device Lett.*, vol. 32, no. 8, pp. 1083–1085, Aug. 2011.

[21] J. Jang, J. Kim, M. Bae, J. Lee, D. M. Kim, D. H. Kim, J. Lee, B.-L. Lee, B. Koo, and Y. W. Jin, "Extraction of the sub-bandgap density-of-states in polymer thin-film transistors with the multi-frequency capacitance-voltage spectroscopy," *Appl. Phys. Lett.*, vol. 100, no. 13, pp. 133506-1–133506-4, Mar. 2012.

[22] K. Jeon, C. Kim, I. Song, J. Park, S. Kim, S. Kim, Y. Park, J.-H. Park, S. Lee, D. M. Kim, and D. H. Kim, "Modeling of amorphous InGaZnO thin-film transistors based on the density of states extracted from the optical response of capacitance-voltage characteristics," *Appl. Phys. Lett.*, vol. 93, no. 18, pp. 182102-1–182102-3, Nov. 2008.

[23] J.-H. Park, K. Jeon, S. Lee, S. Kim, S. Kim, I. Song, C. J. Kim, J. Park, Y. Park, D. M. Kim, and D. H. Kim, "Extraction of density of states in amorphous GaInZnO thin-film transistors by combining an optical charge pumping and capacitance–voltage characteristics," *IEEE Electron Device Lett.*, vol. 29, no. 12, pp. 1292–1295, Dec. 2008.